COMPARISON OF THE CALCULATED NEUTRAL BEAM SHINETHROUGH OF THE WENDELSTEIN VII-A INJECTION WITH CALORIMETRIC MEASUREMENTS

F.-P. Penningsfeld

IPP 4/232 June 1987

MAX-PLANCK-INSTITUT FÜR PLASMAPHYSIK

8046 GARCHING BEI MÜNCHEN

MAX-PLANCK-INSTITUT FÜR PLASMAPHYSIK

GARCHING BEI MÜNCHEN

COMPARISON OF THE CALCULATED NEUTRAL BEAM SHINETHROUGH OF THE WENDELSTEIN VII-A INJECTION WITH CALORIMETRIC MEASUREMENTS

F.-P. Penningsfeld

IPP 4/232 June 1987

Die nachstehende Arbeit wurde im Rahmen des Vertrages zwischen dem Max-Planck-Institut für Plasmaphysik und der Europäischen Atomgemeinschaft über die Zusammenarbeit auf dem Gebiete der Plasmaphysik durchgeführt.

COMPARISON OF THE CALCULATED NEUTRAL BEAM SHINETHROUGH OF THE WENDELSTEIN VII-A INJECTION WITH CALORIMETRIC MEASUREMENTS

F.- P. Penningsfeld

Abstract

Density profiles of the Wendelstein VII-A plasma as measured by Thomson scattering are used to calculate the temporally and spatially varying power density of the neutral beam shinethrough on the torus calorimeter for several shot series. The total energy deposited by the three beam species is obtained by integrating the transmitted power density in space and time. This global quantity is compared with the calorimetric measurements routinely performed for each shot.

The agreement between calculated and measured energy is found to be $\Delta E/E = 2.3 \pm 11$ % confirming the error estimation for the NEUDEN program used, which was only slightly modified to calculate the power density transmitted in the target plane. From this good agreement it is concluded that the program contains a realistic beam model and reliable cross-sections for the beam attenuation which is important for further applications .

Furthermore, the same comparison was done with old results of the ODIN code by analyzing the corresponding raw data as far as they could be recovered, obtaining a similarly good consistency .

A possible increase of 10 to 20 % of the beam stopping cross section which could be expected for Wendelstein VII-A conditions by the effect of multistep collision processes as suggested by Boley et al. /4/ is discussed also.

Table of contents

I. Introduction

There are mainly three reasons for recalculating the neutral beam shinethrough for the Wendelstein VII-A injection more precisely and for verifying the results by measurements :

Firstly, the nearly perpendicular injection geometry and the existence of a torus calorimeter opposite to each injector represent a good experimental setup (see Fig. 1) to examine the shinethrough losses of the neutral beams under very different plasma conditions and to confirm the corresponding results of the NBI codes ODIN /1/ and NEUDEN /3/ experimentally.

Secondly, owing to the geometry mentioned, the shinethrough losses are greater than 40 % in most of the cases and strongly affect the plasma power balances. A carefully tested power deposition code is therefore necessary to provide a reliable data base for the plasma power balance.

Thirdly, a systematic deviation occurring between computed and measured data could be interpreted as the result of multistep collision processes increasing the beam stopping cross-sections as discussed by Boley et al. /4/.

The quantity chosen to be compared was the total energy delivered to the torus calorimeter during an injector pulse since it can be measured directly by recording the temperature rise of the calorimeter plates. This quantity can also easily be calculated by integrating the instantaneous transmitted power density over the target area of the calorimeter for any arbitrarily chosen time point if the plasma density $n_e(\vec{x}, t)$ is known. A second integration of the time-dependent transmitted power $P_S(t)$ gives the total energy delivered to the calorimeter behind the plasma column.

Fig. 1: The Wendelstein VII-A injection system showing the positions of the extraction grid, divided into four segments, the injection duct and the torus calorimeter used for the reported measurements

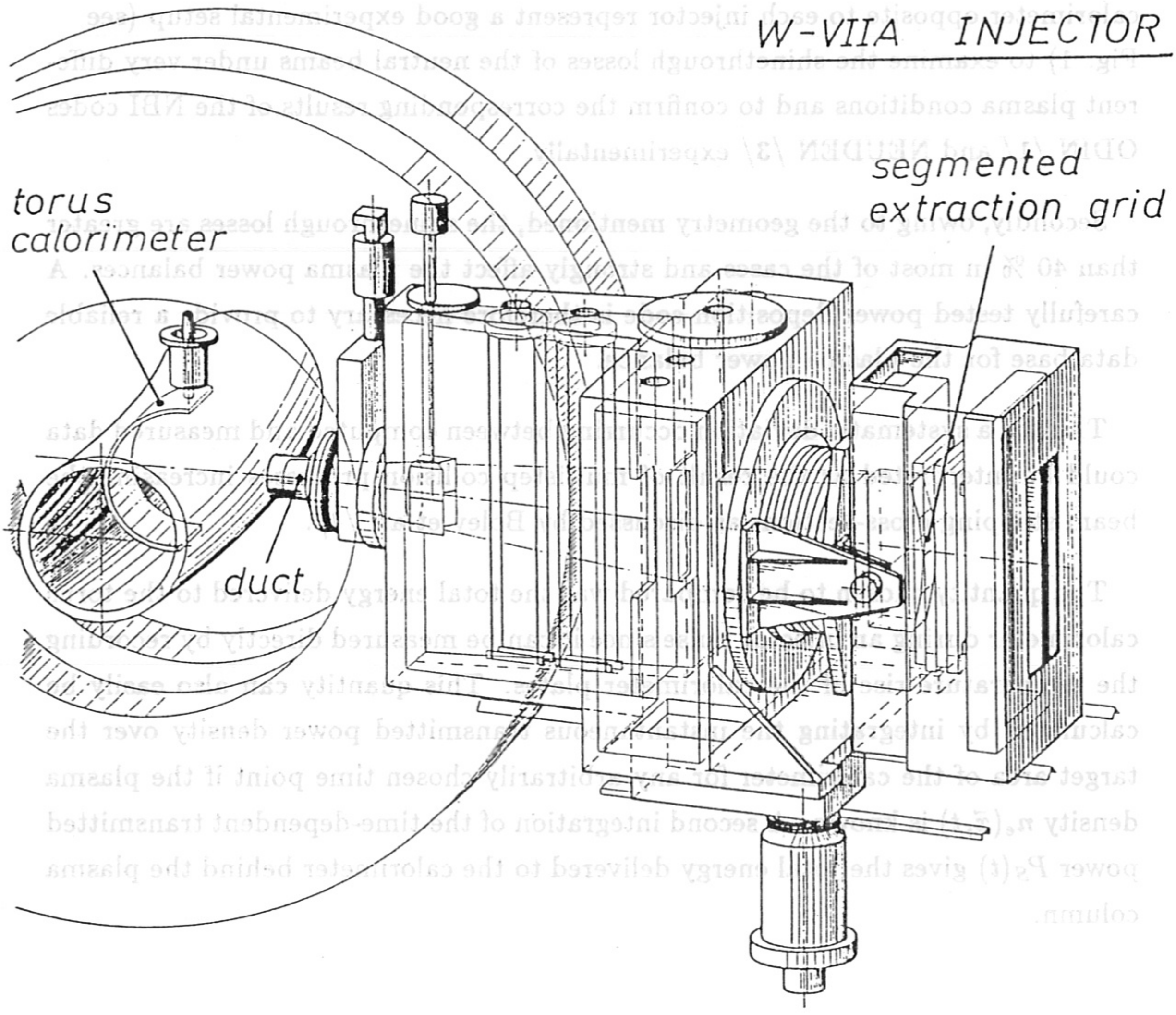

II. Calculation of the shinethrough

The shinethrough varies with the neutral beam parameters and the plasma density, which strongly changes in time during the injection phase. Therefore, even if the neutral beam parameters remain constant during a pulse as shown in reference /5/, the power distribution of the unabsorbed beam impinging on the torus calorimeter behind the plasma column varies in time and space. This quantity $p_S(u,v,t)$ can be calculated stepwise in time for the actual plasma density profile $n_e(\vec{x},t)$ on the target area (u,v) . The integral over the whole calorimeter area (u,v) then gives the instantaneous transmitted power $P_S(t)$. The total energy given by

$$E_{cal} = \int_{t_i}^{t_f} P_S(t)dt \tag{1}$$

is then compared with the calorimetric measurement.

II.1 The program used

For the calculation of $P_S(t)$ the NEUDEN program /3/ was used with the following modifications :

i) Instead of the particle density of fast neutrals, now the power density of the neutral beam after its passage through the plasma column is summed up over all beamlets of the source for each species separately, giving the power density distribution $p_S(u,v,t)_i$ for each species i (see Fig.3, for example).

ii) This distribution $p_S(u,v,t)_i$ is integrated over the calorimeter area to give the instantaneous transmitted power $P_S(t)_i$ for each species.

iii) The total instantaneous transmitted power $P_S(t)$ is the sum over the three contributions $P_S(t)_i$, with $i = 1,2,3$.

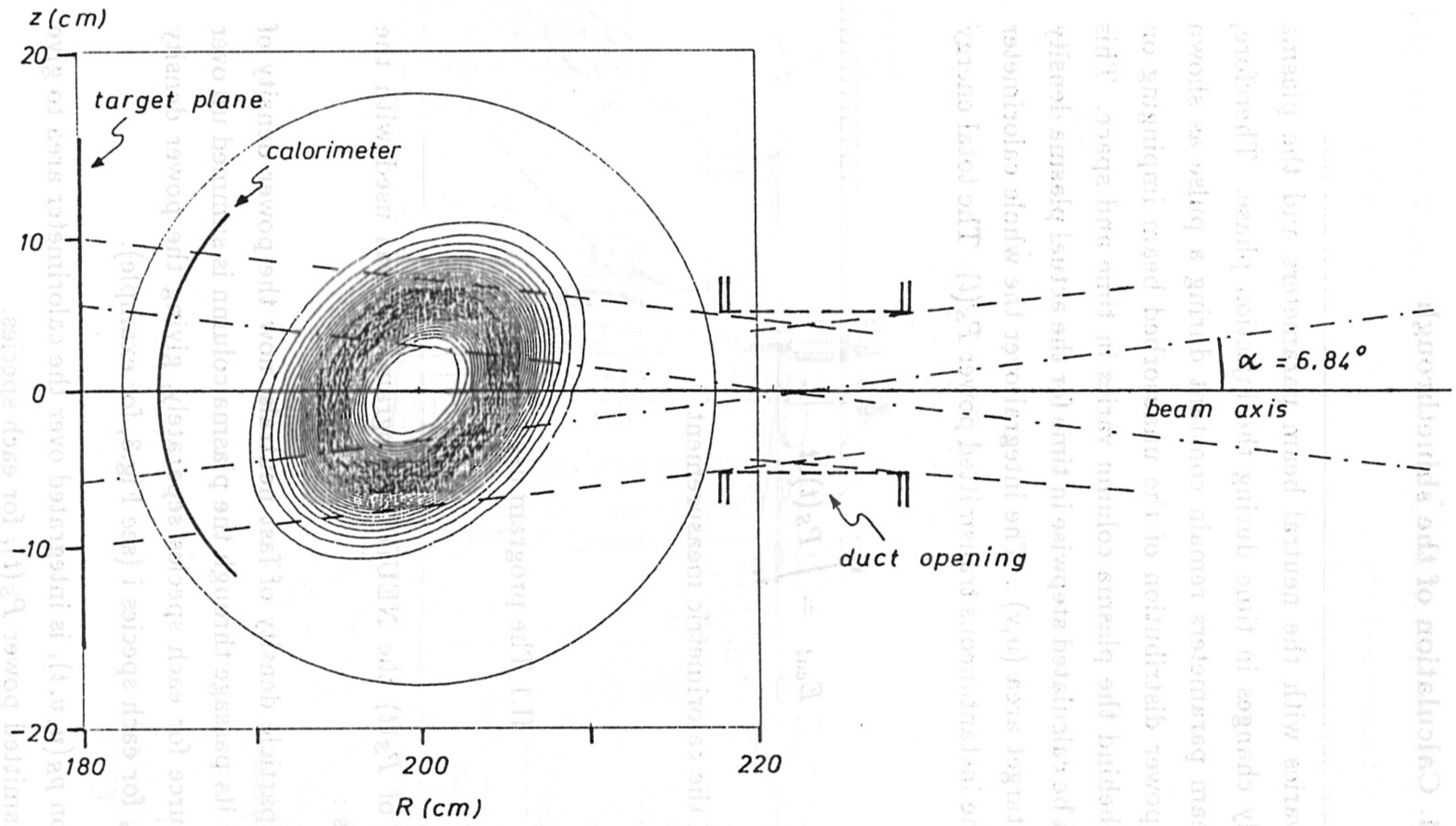

Fig. 2: Injection geometry projected into the poloidal plane showing the positions of the target plane and the two scrapers simulating the entrance duct used in the modified NEUDEN code. The plasma position is displayed by the plot of the density profile valid for the series A at $t_0 = 230$ ms.

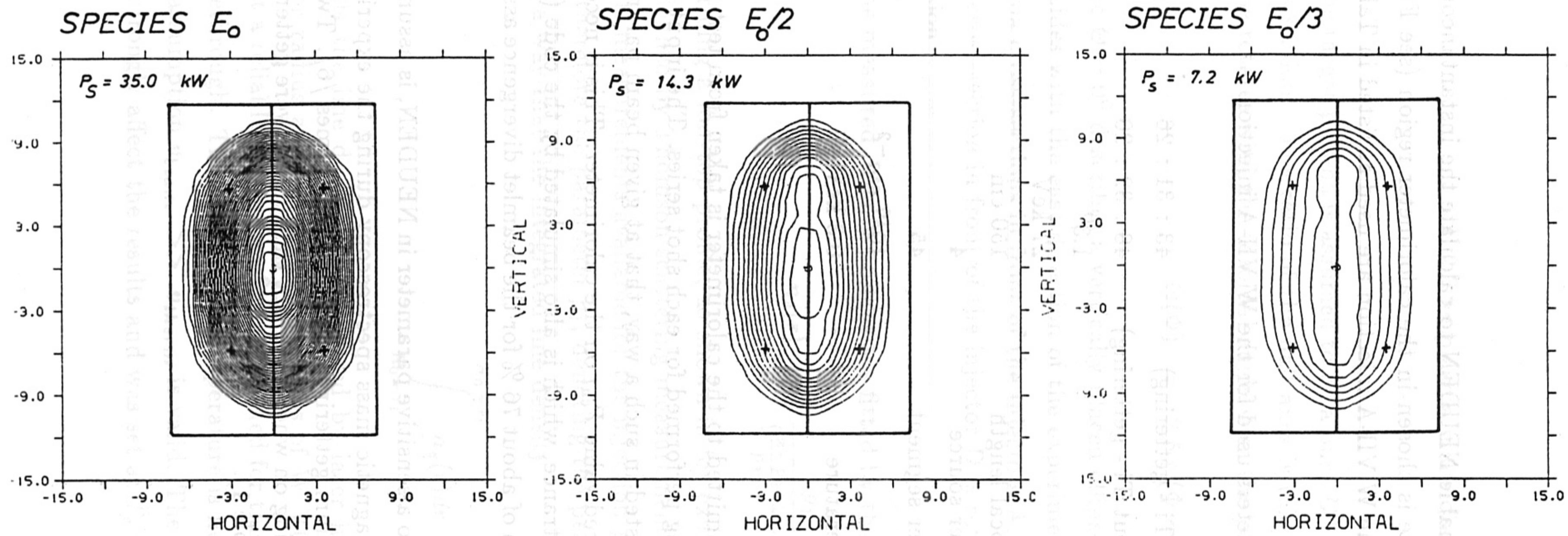

Fig. 3: Power density transmitted to the torus calorimeter calculated by NEUDEN for series A at $t_0 = 230$ ms. The two calorimeter plates are indicated by rectangles. The full energy component contributes a peak density of 420 $W cm^{-2}$

These minor modifications enable NEUDEN to calculate the instantaneous shinethrough if the target plane is chosen in the calorimeter region (see Fig. 2) and the input parameters for the W VII-A injection are used as listed in Table 1 .

Table 1 : Beam parameters used for the W VII-A injection

ion species mix (with Ti - gettering)	43 : 31 : 26
ion species mix (without Ti - gettering)	48 : 32 : 20
beamlet divergence	1.3^0
beam energy	27 keV
horizontal and vert. focal length	150 cm
number of segments per source	4
number of beamlets per segment	45
neutraliser target	10^{16} cm^{-2}
plasma electron temperature	0.3 keV

The neutral power P_{cal} transmitted to the calorimeter is taken from test pulses without plasma discharges being performed for each shot series. The input power P_N needed for the code is adjusted in such a way, that at given beam parameters the code reproduces the measured value P_{cal} on the calorimeter. This is necessary because the very small duct entrance, which is also simulated by the code (see Fig. 2), only has a transmission of about 76 % for the beamlet divergence assumed.

The species mix, which is also a sensitive parameter in NEUDEN, is assumed to be the same as measured by magnetic mass spectroscopy during the experiments for analyzing the effect of titanium gettering of the source volumes /6/. Two sets of species mix are used depending on whether or not the sources were gettered for the shot series treated (see Table 1).

II.2 The plasma model for W VII-A

The target plasma is assumed to be a pure D^+ or He^{++} plasma with an elliptic cross-section . The ratio of the half axes is taken to be $a/b = 0.70$. The plasma ellipse rotates with the toroidal angle Φ in the poloidal direction Θ according to

$$\Theta(\Phi) = 2.5 * (\Phi - 18^0) \tag{2}$$

where $\Theta = 0^0$ describes a vertically placed ellipse at $\Phi = 18^0$. The value $\Phi = 0^0$ coincides with the east direction of the experiment. The resulting position of the plasma cross-sections in front of the injectors A, B and C is depicted in Fig. 1b. The cross-section in front of the injector D is rotated by 90^0 with respect to this position .

The measured density profiles are fitted by the expression

$$n_e(r) = \frac{p_1}{(\frac{x-p_2}{p_3})^{2p_4} + 1} \tag{3}$$

describing a flat-top profile, as shown in for example Fig. 4. The parameters p_i are defined by Thomson scattering measurements. But there are only one or two profile measurements available for the injection phase of the shots treated so far, and therefore the parameter p_1, denoting the peak plasma density, is adjusted in such a way that the integrated line density

$$\int_{R_0-r_l}^{R_0+r_l} n_e(r)dr \tag{4}$$

equals the line density as measured by laser interferometry . R_0 denotes the major radius and r_l the limiter radius of W VII-A. In this way, for every time point a reliable density profile is obtained for the calculation of the instantaneous shinethrough. The plasma ion temperature is neglected, because for $\bar{T}_i \leq 1keV$ the assumption $v_{beam} >> v_{therm}$ is valid. The mean electron temperature does not strongly affect the results and was set at $\bar{T}_e = const. = 300\ eV$.

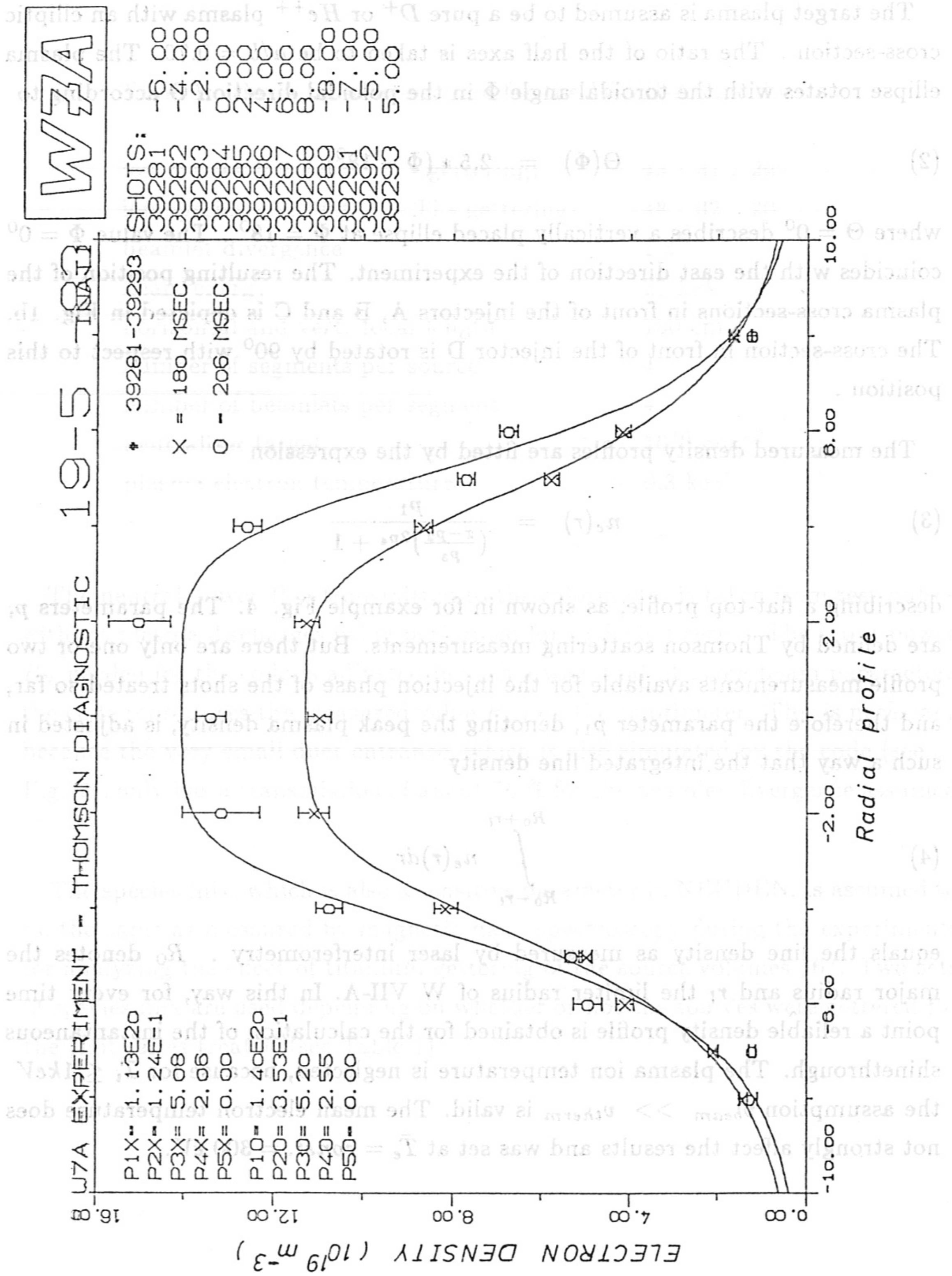

Fig. 4: Example for the electron density profiles used for the shinethrough calculations (series A, two timepoints). The parameters according equ.(3) are indicated also.

II.3 The beam attenuation

The code uses analytical representations of the cross-sections for the beam attenuation by charge exchange and ion and electron impact ionisation given by Galbraith and Kammash /7/ (see also /3/). The resulting total cross-section for $T_e = 1.0$ keV and $Z_{eff} = 1$ is shown in Fig. 5 (dashed line). The contribution of excited atoms generated by multistep collisions of the beam particles should increase the total cross-section as discussed by Boley et al. /4/ depending mainly on the parameters beam energy, plasma density and Z_{eff}. For comparison the cross-sections with and without the contribution of the multistep collision processes are plotted also in Fig. 5. The agreement between the used fit and the reported values without excitations is very close below 10 keV/amu . In the range $10 \leq E_0 \leq 150$ keV/amu a difference of about 10 % occurs due to different fits to the cross-section data falling well below the usual experimental error.

Fig. 5: Comparison of the beam attenuation cross-sections

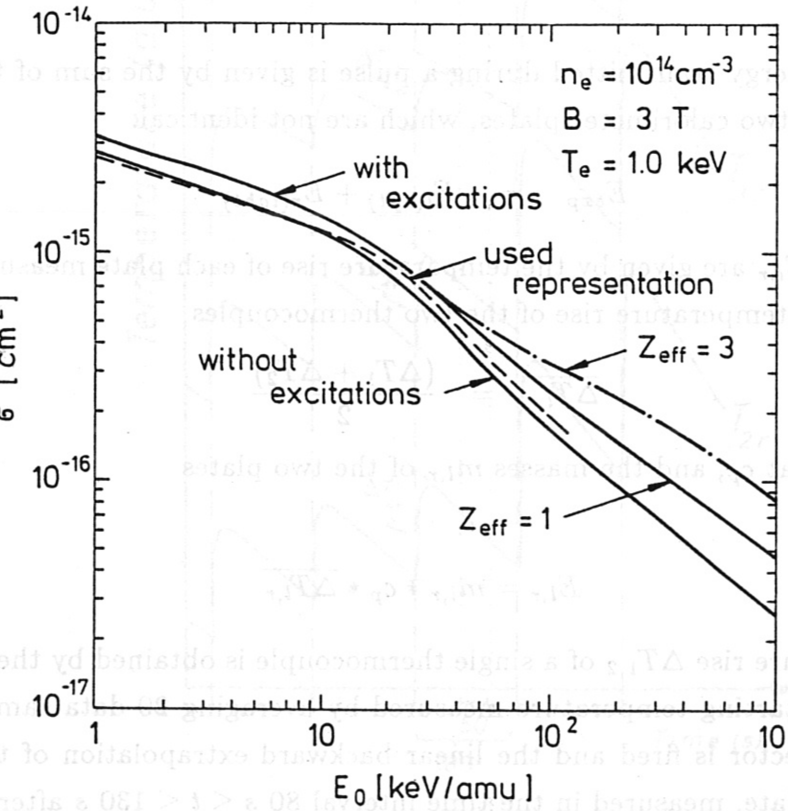

III. Calorimetric measurements

III.1 The torus calorimeter in W VII-A

The shinethrough of each of the four neutral beams on W VII-A is measured by a calorimeter mounted on the inner wall of the torus opposite to the injector (see Fig. 1). It consists of two 5 mm thick curved molybdenum plates which are vertically separated. Each of them supports two thermocouples mounted $\pm$ 6.0 cm apart from the horizontal plane. The total area of the calorimeter projected into a plane vertical to the beam axis is about 14.5 $*$ 23.5 cm^2, which stops the whole beam transmitted through the nearly elliptic duct opening with half axes $a = 4.2\ cm$, $b = 4.7\ cm$.

III.2 Evaluation of the calorimetric data

The total energy transmitted during a pulse is given by the sum of the contributions of the two calorimeter plates, which are not identical:

(5) $$E_{exp} = E_{l(eft)} + E_{r(ight)}$$

The energies $E_{l,r}$ are given by the temparature rise of each plate measured by the average of the temperature rise of the two thermocouples

(6a) $$\overline{\Delta T_{l,r}} = \frac{(\Delta T_1 + \Delta T_2)}{2}$$

the specific heat c_p, and the masses $m_{l,r}$ of the two plates

(6b) $$E_{l,r} = m_{l,r} * c_p * \overline{\Delta T_{l,r}}$$

The temperature rise $\Delta T_{1,2}$ of a single thermocouple is obtained by the difference between the starting temperature measured by averaging 20 data samples taken before the injector is fired and the linear backward extrapolation of the cooling curve of the plate, measured in the time interval 80 $s \le t \le$ 130 s after the shot.

Fig. 6: Example of the four thermosignals of the torus calorimeter of injector A used for determining the transmitted energy. For shot 39293 the determination of the temperature rise is illustrated also. TEST1 and TEST2 denote the signals of two consecutive test pulses without plasma.

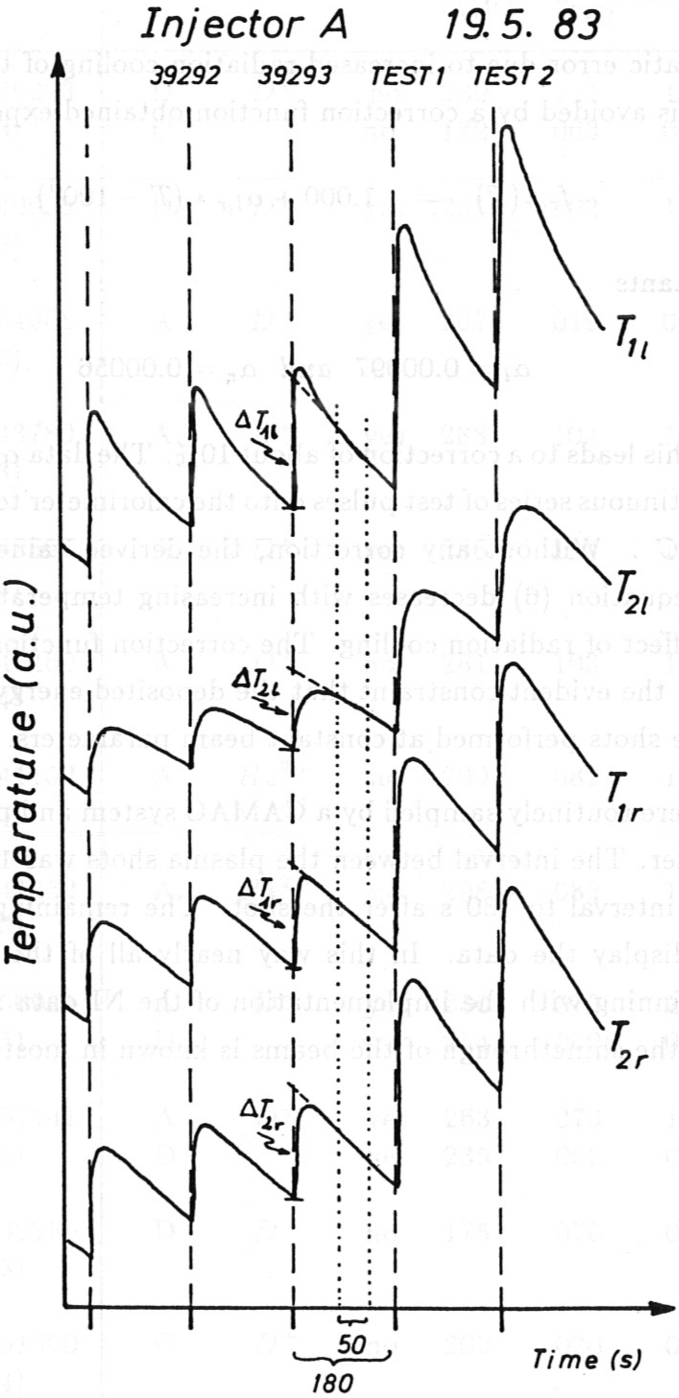

Figure 6 shows the typical signals of the four thermocouples of one calorimeter. The monotonic decrease of the cooling curves in the measuring interval justifies the implicit assumption of equation (6) that the plates have reached their thermal equilibrium. The estimated error of this method due to data noise and digital resolution is about 8%.

The systematic error due to increased radiation cooling of the plates at higher temperatures is avoided by a correction function obtained experimentally:

$$(7a) \qquad f_{cor}(T) = 1.000 + \alpha_{l,r} * (T - 100^0)$$

with the constants

$$(7b) \qquad \alpha_l = 0.00097 \quad and \quad \alpha_r = 0.00056$$

At $T = 200^0$ this leads to a correction of about 10%. The data $\alpha_{l,r}$ were determined by firing a continuous series of test pulses onto the calorimeter to heat it from about 25^0C to 250^0C . Without any correction, the derived value for the deposited energy after equation (6) decreases with increasing temperatures of the plates, showing the effect of radiation cooling. The correction function of equation (7) is obtained from the evident constraint that the deposited energy must be the same for all of these shots performed at constant beam parameters.

The data were routinely sampled by a CAMAC system and processed by a PDP 11/45 computer. The interval between the plasma shots was 180 s, which limited the sampling interval to 130 s after the shot. The remaining time was used to process and display the data. In this way nearly all of the plasma shots were recorded, beginning with the implementation of the NI data acquisition early in 1982, so that the shinethrough of the beams is known in most cases.

Table 2 : Compilation of the analyzed shot series
A-L : H^0-injection
X : D^0-injection

Name	Shots (Date)	Inj.	Plasma	Titan	P_{cal} (kW)	t_p (ms)	E_{cal} (kJ)	E_{exp} (kJ)	$\frac{\Delta E}{E_{exp}}$ %
A	39281- 39293 (19.05.83)	D C	D^+	no no	239 172	111 063	10.48 03.34	10.40 03.78	+00.8 -11.6
B	40884- 40938 (20.07.83)	D	D^+	yes	261	102	14.56	14.60	-00.3
C	34065- 34068 (04.08.82)	A	D^+	yes	207	019	01.89	02.10	-10.0
D	43757- 43780 (07.12.83)	A	D^+	yes	288	104	15.66	17.80	-12.0
E	43873- 43897 (12.12.83)	A	D^+	yes	286	124	19.90	19.42	+02.5
F	47433- 47460 (02.04.84)	A	D^+	no	281	103	16.38	15.32	+06.9
G	41128- 41152 (25.07.83)	A	He^{2+}	no	299	082	15.81	15.91	-00.6
H	41212- 41252 (27.07.83)	A	He^{2+}	no	298	082	17.28	15.20	+13.7
I	56907- 56921 (19.04.85)	A D	D^+	yes yes	250 254	073 062	10.21 07.77	08.70 06.48	+17.3 +19.5
K	57127- 57141 (22.04.85)	A D	D^+	yes yes	263 235	073 062	11.79 08.49	10.65 07.70	+10.7 +10.3
L	38341- 38386 (29.04.83)	D	D^+	no	175	070	03.61	03.75	-03.7
X	51313- 51320 (20.07.84)	C	D^+	no	202	020	01.36	01.57	-13.3

IV. Comparison of the results

Up to five separate code runs were done for each heating pulse analyzed to get a good picture of the time-varying transmitted power. This amount of work limits the number of shots compared. Only a small set of series labelled A - L is therefore treated to check the NEUDEN code for H^0-injection. One example of D^0-injection is analyzed in series X.

Short 'diagnostic pulses' of 20 ms duration, fired at different time points of the discharge, are treated in series M and N. They give a more or less instantaneous measure of the shinethrough . Furthermore the total neutral energy of this injector transmitted to the torus can be obtained by the extrapolation of the experimental data to the limit $\int ndl \rightarrow 0$ as an alternative to the usual power estimation by a separate testpulse.

Additionally, the ODIN results for the shinethrough previously reported /1/ are compared with the experiment . For this purpose the existing raw data had to be evaluated afterwards by the same method as mentioned above , because the data acquisition system did not exist at that time.

VI.1 Results for heating pulses

Table 2 lists the analyzed shot series for heating pulses with their main parameters. These series are selected according to the following criteria :

i) At least one n_e profile measurement during the NI phase is available

ii) A successful test pulse for the beam power of the injector without plasma exist

iii) NI data acquisition works properly

iiii) The whole injection scenario should be treated :
e.g. low and high-density discharges, D^+ and He^{++} discharges, pellet injection during NI , short and long injection pulses and combined heating with ECRH and NI.

Figures 7 a-k give the time-dependent power $P_S(t)$ impinging on the torus calorimeter for one and two injectors for the shot series listed in Table 2 as calculated by the modified NEUDEN code. For comparison reasons the plot of the line density measured by laser interferometry is also given. The interpolation between the calculated points is done strictly in accordance with the variation of this line density integral. The total energy is obtained by integration of these $P_S(t)$ curves over the whole injector pulse .

Figure 8 shows the correlation between the measured energy and the calculated energy. The error bars correspond to the estimated error of the experimental data. The subsequently analysed shots, the shinethrough of which was calculated earlier by using the ODIN code /1/, are also included in the diagram (without error bars). For one of the shots reported in Ref. /1/, it was no longer possible to achieve a complete reconstruction of the data set, and so this shot was omitted. The maximal deviations from the ideal correlation $E_{cal} = E_{exp}$ (see dashed line in Fig. 8) found so far for the results of the modified NEUDEN code may be described by their mean value and its standard deviation given by

$$(8) \qquad \overline{\left(\frac{\Delta E}{E_{exp}}\right)} = \overline{\left(\frac{E_{cal} - E_{exp}}{E_{exp}}\right)} = 2.3 \pm 11 \ \%.$$

This falls well below the estimated error range of 20% for this code /3/ and does not show a significant systematic effect. The exact numbers are given in Table 2.

Fig 7a **Line density measured by laser interferometry for shot series A and transmitted power $P_S(t)$ calculated for injectors C and D. The density increase at $t = 162$ ms is caused by pellet injection.**

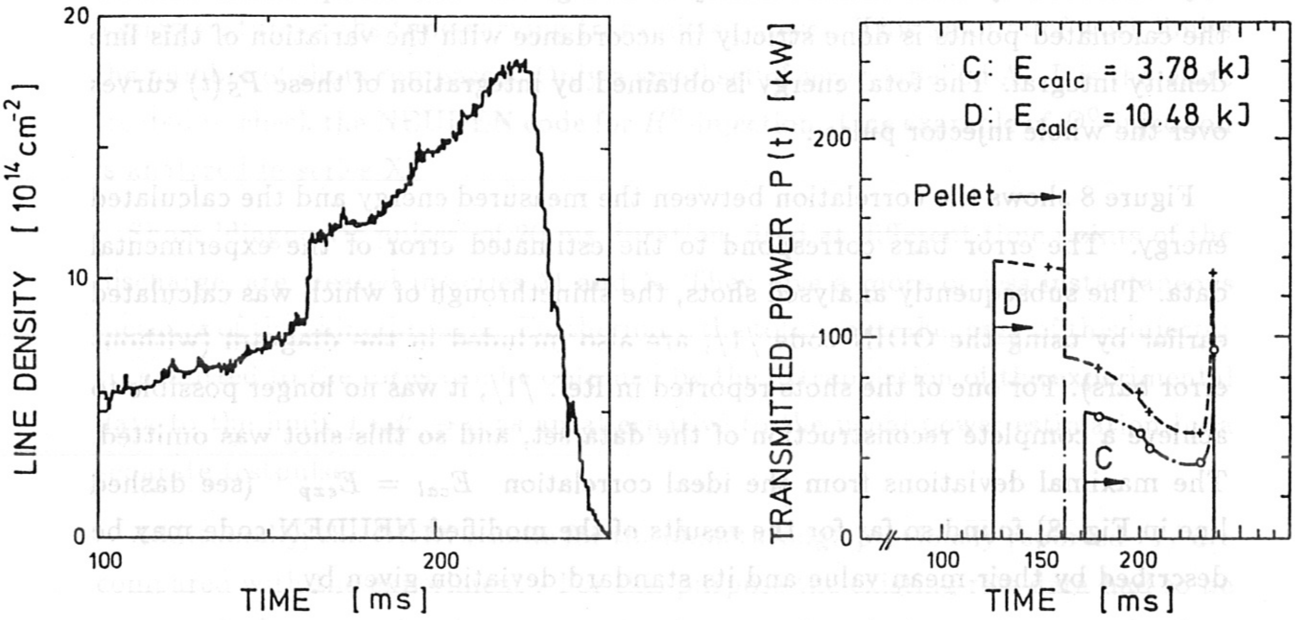

Fig 7b: **Line density and transmitted power as calculated by NEUDEN for series B, injector D.**

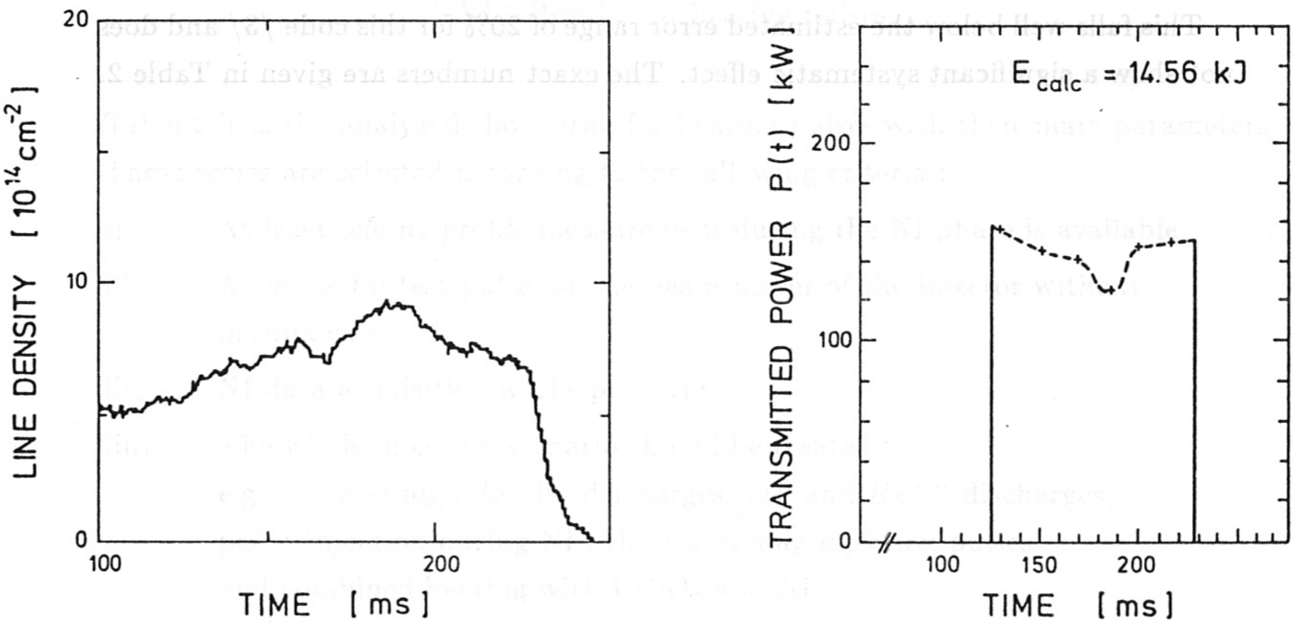

Fig 7c: Line density and transmitted power as calculated by NEUDEN for series C, injector A. Example of a short injector pulse.

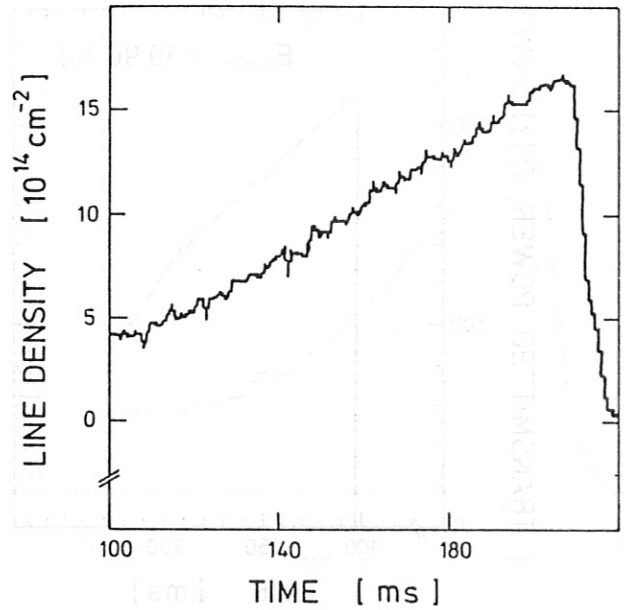

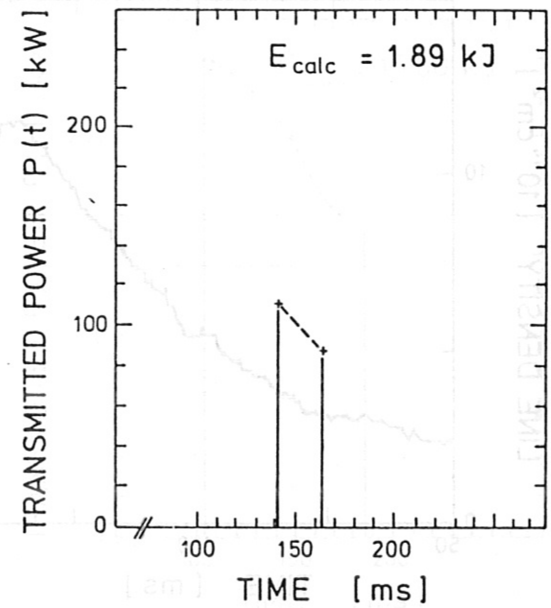

Fig 7d: Line density and transmitted power as calculated by NEUDEN for series D, injector A.

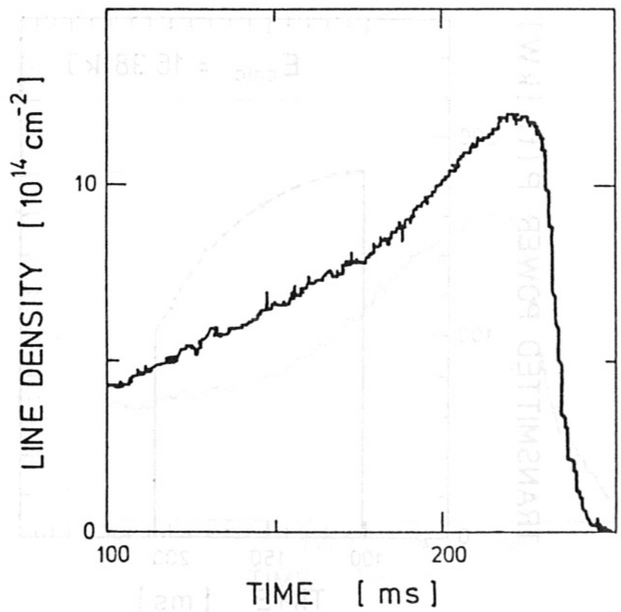

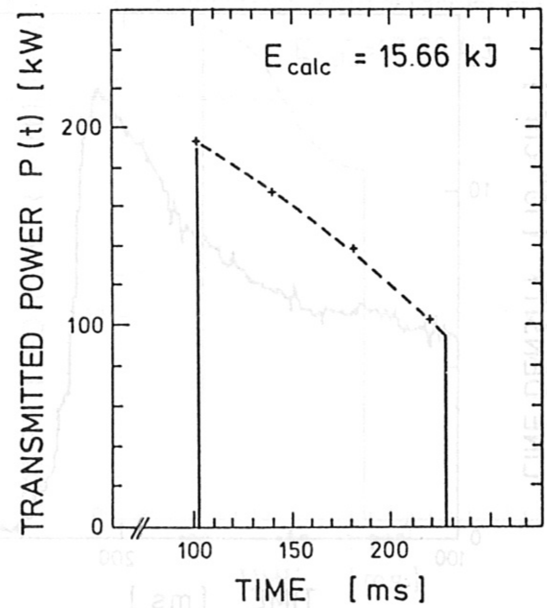

Fig 7e: Line density and transmitted power as calculated by NEUDEN for series E, injector A.

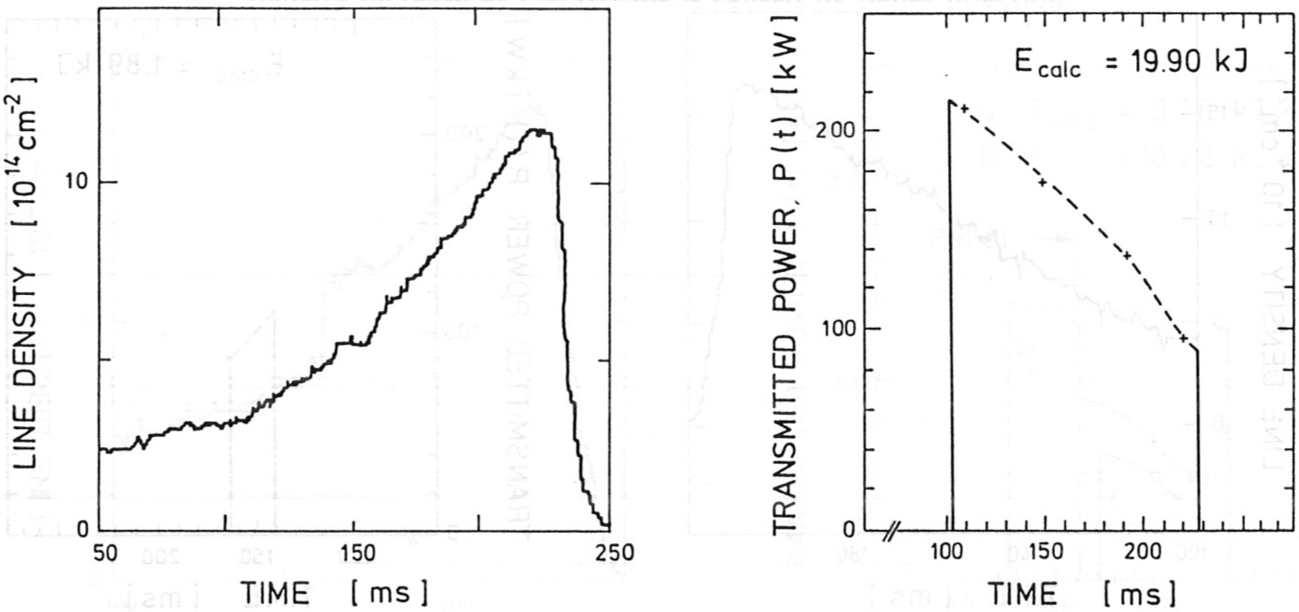

Fig 7f: Line density and transmitted power as calculated by NEUDEN for series F, injector A.

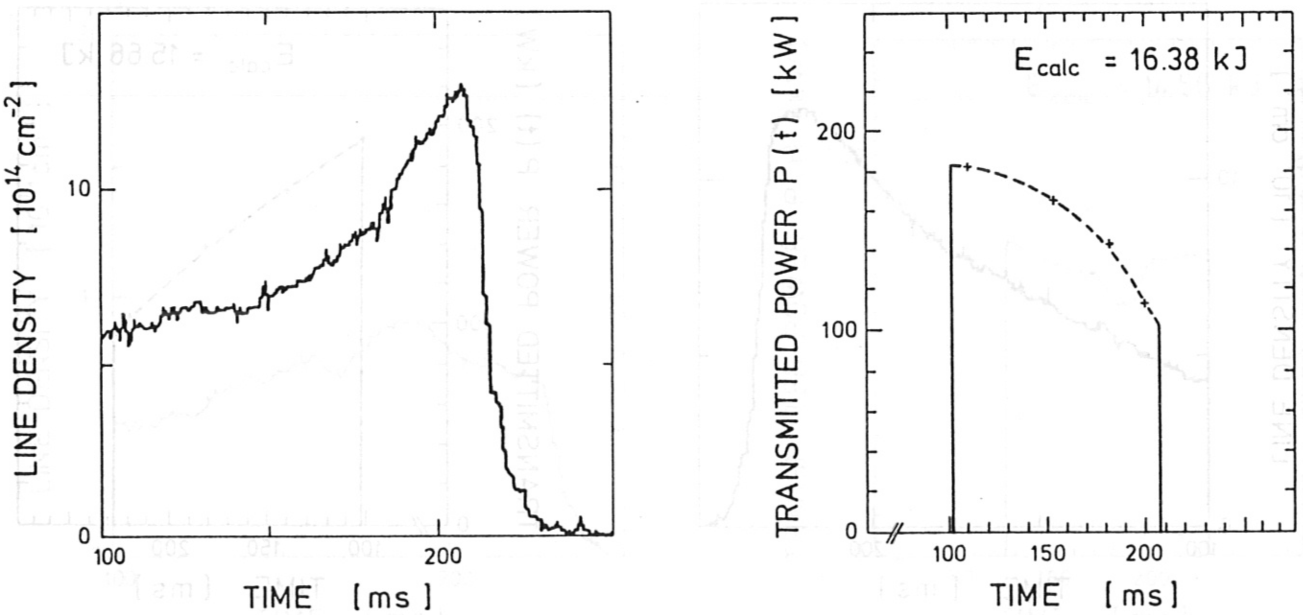

Fig 7g: Line density and transmitted power as calculated by NEUDEN for series G, injector A. Example of a helium discharge.

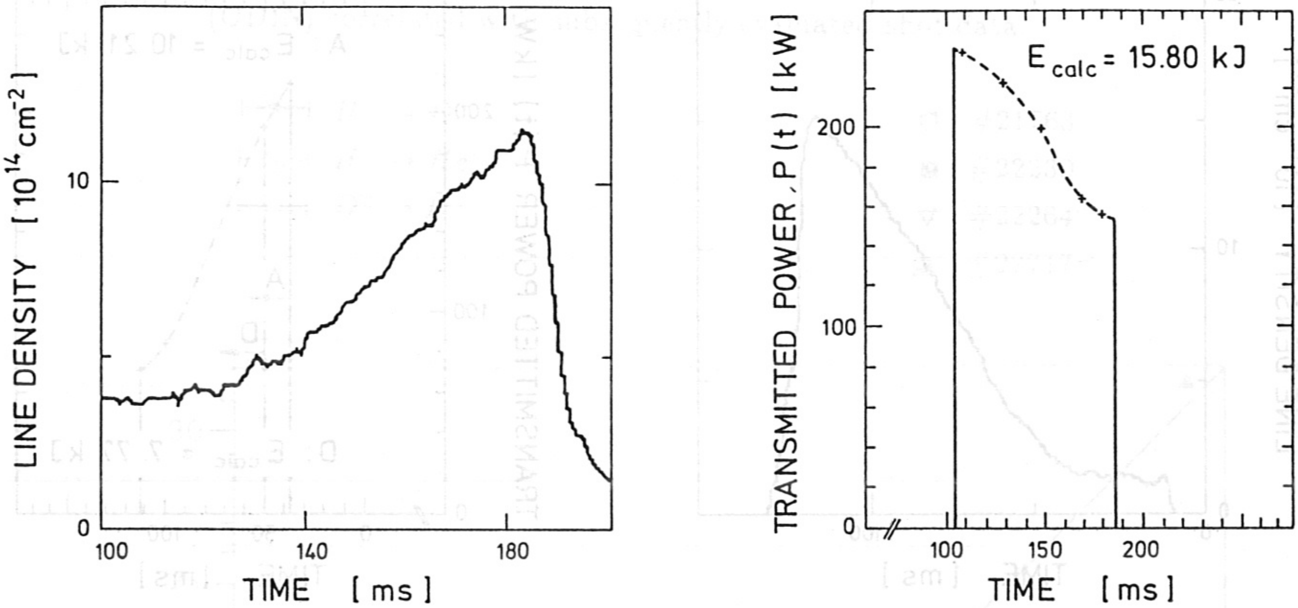

Fig 7h: Line density and transmitted power as calculated by NEUDEN for series H, injector A. Example of a helium discharge.

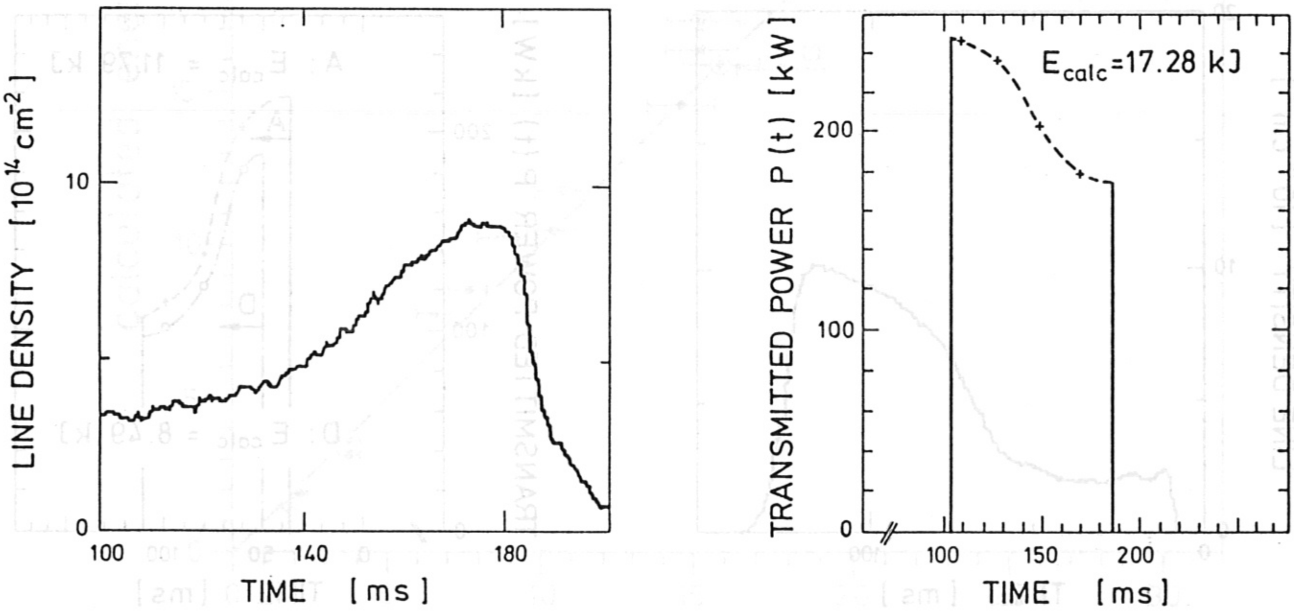

Fig 7i: Line density and transmitted power as calculated by NEUDEN for series I, injectors A and D. This is an example of combined ECRH and NI heating.

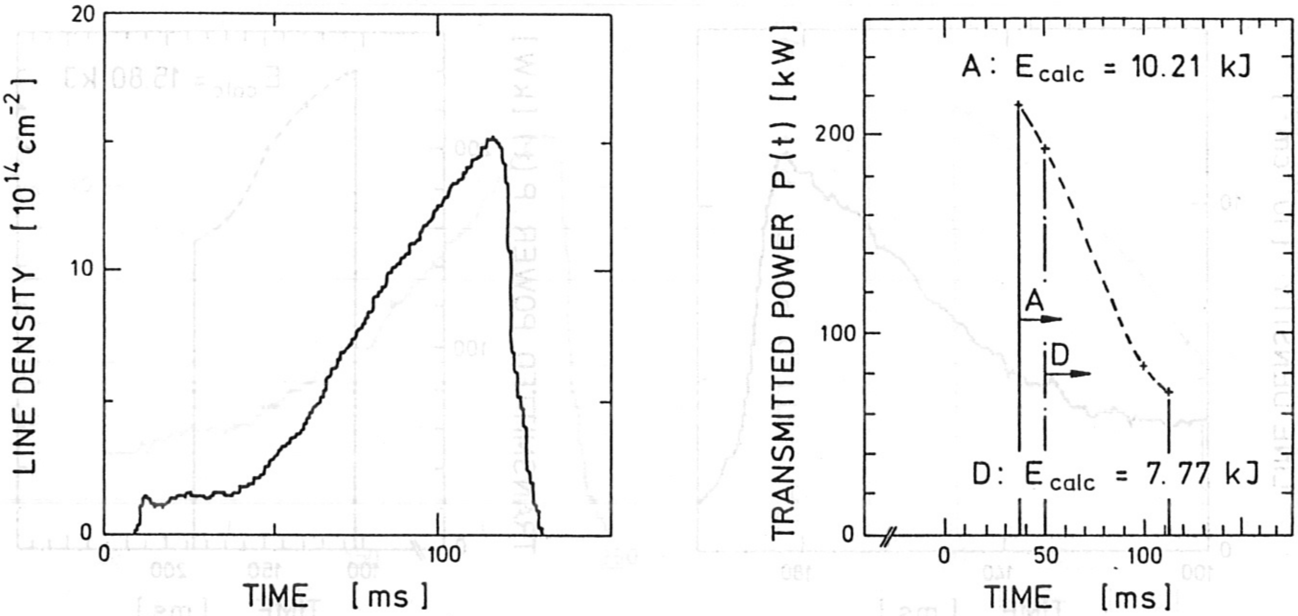

Fig 7k: Line density and transmitted power as calculated by NEUDEN for series K. This is another example of combined ECRH and NI heating.

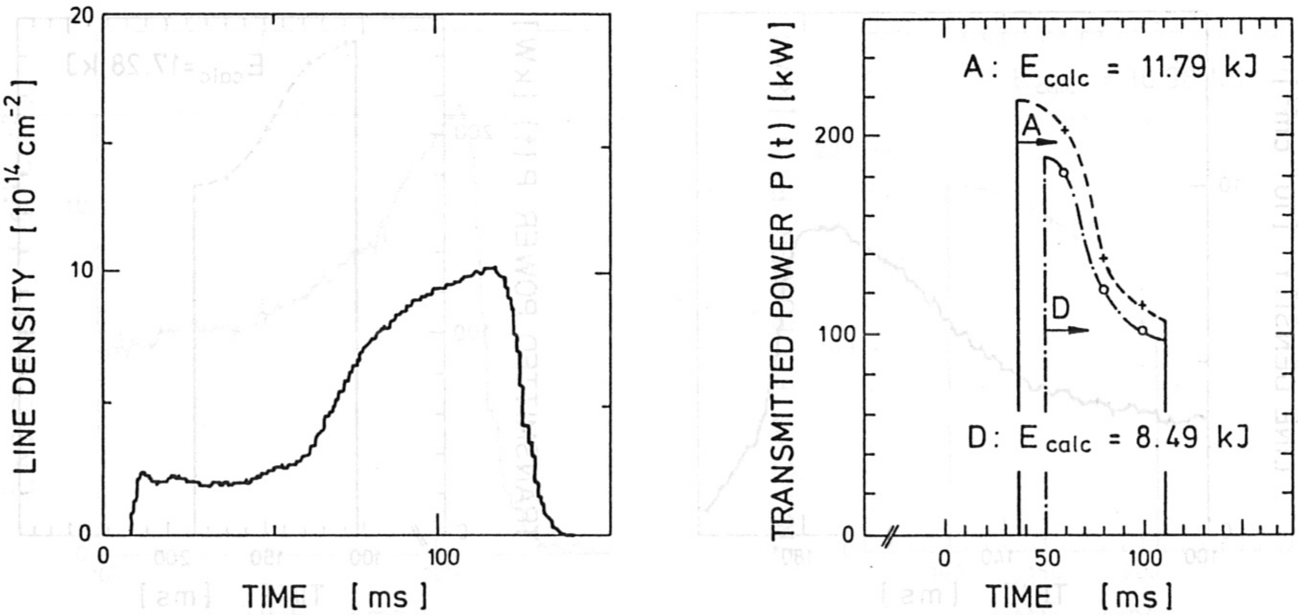

Fig. 8: Correlation between the measured energy E_{exp} on the torus calorimeter and the energy E_{cal} calculated by NEUDEN. The points without error bars show the results of older shinethrough computations (ODIN) correlated with subsequently evaluated shot data.

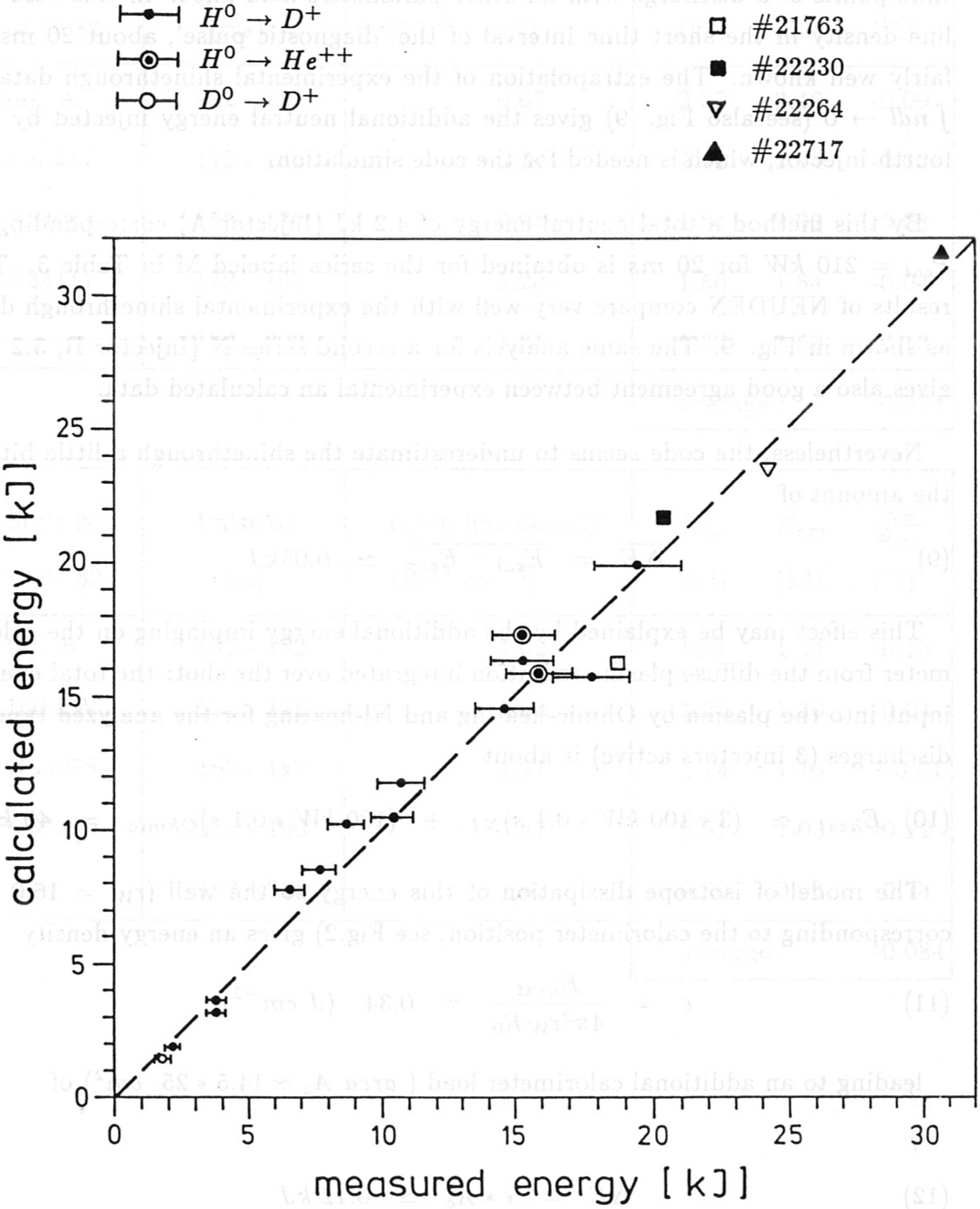

VI.2 Results for diagnostic pulses

A nearly instantaneous measurement of the shinethrough can be done by the use of the fourth injector as a diagnostic beam: a short pulse is fired at different time points of a discharge with all other parameters held fixed. In this case the line density in the short time interval of the 'diagnostic pulse', about 20 ms, is fairly well known. The extrapolation of the experimental shinethrough data to $\int ndl \rightarrow 0$ (see also Fig. 9) gives the additional neutral energy injected by the fourth injector, which is needed for the code simulation.

By this method a total neutral energy of 4.2 kJ (Injector A) corresponding to $P_{cal} = 210\ kW$ for 20 ms is obtained for the series labeled M in Table 3. The results of NEUDEN compare very well with the experimental shinethrough data as shown in Fig. 9. The same analysis for a second series N (Injector B, 3.2 kJ) gives also a good agreement between experimental an calculated data.

Nevertheless, the code seems to underestimate the shinethrough a little bit by the amount of

$$(9) \qquad \overline{\Delta E} = \overline{E_{cal} - E_{exp}} \simeq 0.08kJ$$

This effect may be explained by the additional energy impinging on the calorimeter from the diffuse plasma radiation integrated over the shot: the total energy input into the plasma by Ohmic-heating and NI-heating for the analyzed type of discharges (3 injectors active) is about

$$(10) \quad E_{heat} \simeq (3 * 100\ kW * 0.1\ s)_{NI} + (100\ kW * 0.1\ s)_{Ohmic} = 40\ kJ$$

The model of isotrope dissipation of this energy to the wall ($r_W = 16.0\ cm$ corresponding to the calorimeter position, see Fig.2) gives an energy density

$$(11) \qquad \epsilon = \frac{E_{heat}}{4\pi^2 r_W R_0} = 0.34 \quad (J\ cm^{-2})$$

leading to an additional calorimeter load ($area\ A_c \simeq 14.5 * 25\ \ cm^2$) of

$$(12) \qquad \Delta E = \epsilon * A_c \simeq 0.12\ kJ$$

Table 3: Results for two series with short diagnostic pulses ($H^0 \rightarrow D^+$, $t_p = 20\ ms$) produced by the fourth injector at different time points of the discharge

Serie M 04.08.82	Pulse on (ms)	mean line density ($10^{15}\ cm^{-2}$)	E_{cal} (kJ)	E_{exp} (kJ)	$\frac{\Delta E}{E_{exp}}$ (%)
Inj. A	132 - 152	0.67	2.37	2.46	-0.09
210 kW	142 - 162	0.79	2.11	2.14	-0.03
#34054-	152 - 172	0.94	1.84	2.02	-0.08
#34117	172 - 192	1.20	1.50	1.54	-0.04
	182 - 202	1.31	1.37	1.50	-0.13
			average :		-0.074

Serie N 12.07.82	Pulse on (ms)	mean line density ($10^{15}\ cm^{-2}$)	E_{cal} (kJ)	E_{exp} (kJ)	$\frac{\Delta E}{E_{exp}}$ (%)
Inj. B	132 - 152	1.02	1.31	1.44	-0.13
160 kW	152 - 172	1.08	1.26	1.30	-0.04
#33078-	162 - 182	1.21	1.14	1.13	+0.01
#33099	170 - 190	1.47	0.91	1.03	-0.12
	182 - 202	1.62	0.80	0.94	-0.14
			average :		-0.084

Fig. 9:

Measured and calculated shinethrough energy E_S of the 'diagnostic pulse' for different time points, i. e. mean line densities, during two sets of W VII-A discharges with NI - heating by 3 injectors. Independent of the actual line density, the calculated values are found to be somewhat smaller ($\simeq$ 0.08 kJ) than the experimental results. This may be caused by additional energy from the plasma impinging on the calorimeter during the discharge (see text for explanation).

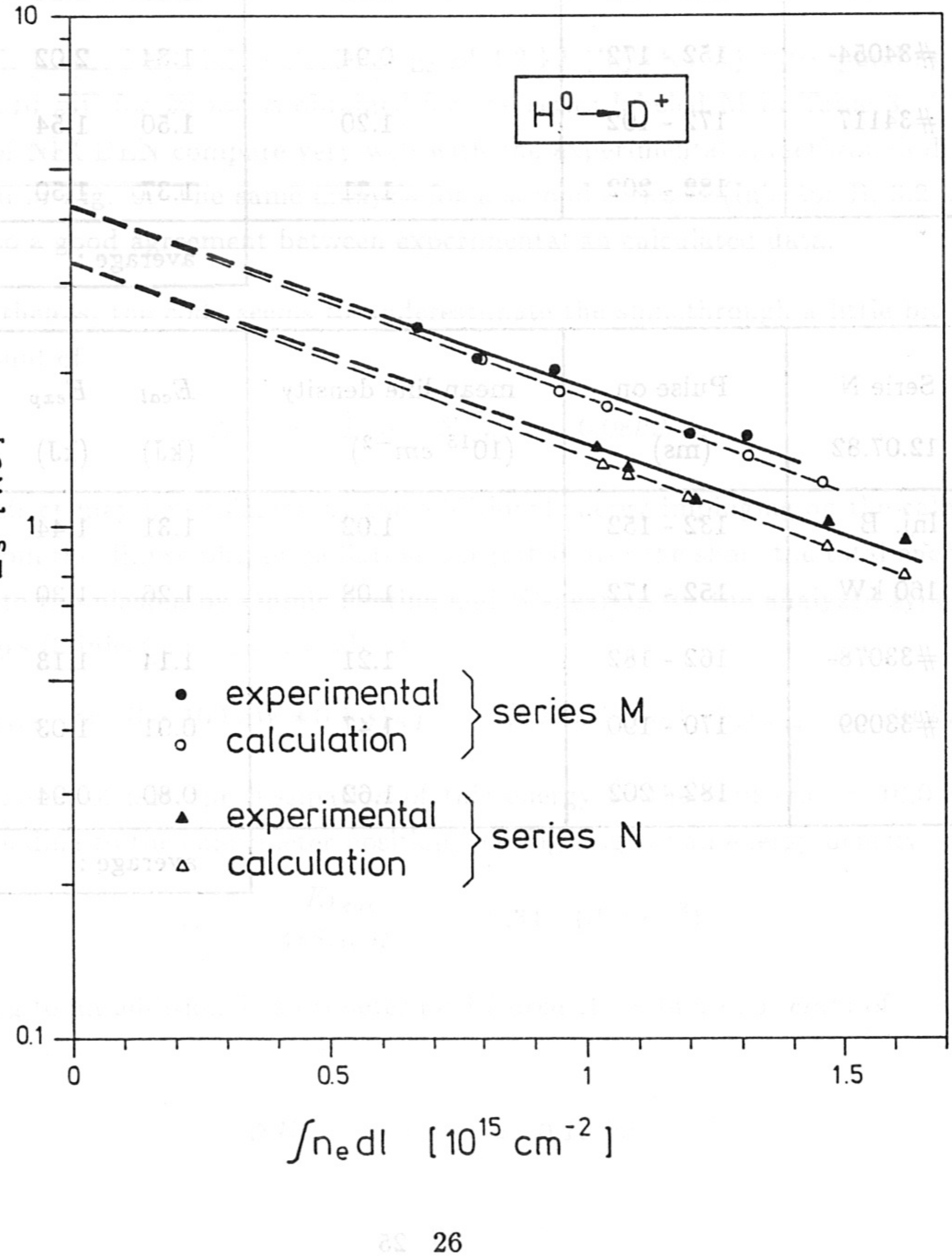

This estimation is very close to the observed systematic deviation of $\overline{\Delta E} = 0.08 kJ$. If this effect is taken into account for the short diagnostic pulses, an even better correlation between measurement and calculation can be obtained.

It should be mentioned, that in the case of the analyzed heating pulses (chapter IV.1) such a small energy deposit cannot be detected, because it is masked by the additional experimental error introduced by the testpulse evaluation.

IV.3 Discussion

The agreement between measured and calculated energy values is found to be very good despiteof the selection of a wide variety of target plasma conditions. This also holds for the old shinethrough calculations with the ODIN code that were usually applied to compute the plasma power balances /2/. Errors of the order of 10% in the calculations are easily explained by changing the species mix or beam divergence during the long-term source operation. Nevertheless this good agreement could be achieved with one single set of beam parameters with the exceptions of the separately measured beam power and the two sets of species mix for gettered and ungettered sources.

A possible increase of the total cross sections of the order

$$(13) \qquad \delta = \frac{\Delta\sigma}{\sigma} = \frac{\sigma' - \sigma}{\sigma}$$

by the contribution of excited atoms produced by multistep collisions as discussed by Boley et al./4/ should result in a variation of the quantity $\Delta E / E_{exp}$ (see Fig. 10):

$$(14) \qquad \frac{\Delta E}{E_{exp}} = e^{\int (\sigma' - \sigma) n_e dl} - 1 = e^{\delta \, \sigma \int n_e dl} - 1$$

The expected systematic increase by such an effect for W VII-A conditions given by equation (14) is plotted in Fig. 10 for $\delta = 10\%$ and 20%. For comparison the obtained results of the heating pulses are plotted versus the time-averaged line density to account for the strong increase of the plasma density during the neutral-beam injection phase. The horizontal bars indicate the line density variations during the calorimetric measurement.

The values for 'diagnostic pulses' are also given in Fig. 10 at their corresponding mean line density during the pulse (see also table 3). They reveal a much smaller error spread due to the elimination of the additional testpulse error by the extrapolation method described in chapter IV.2 .

Fig. 10: Relative deviation between calculation and experiment versus time-averaged line density. The effect of multistep collisions on the neutral beam shinethrough in W VII-A is estimated according to equation 14 for two values of the parameter δ .

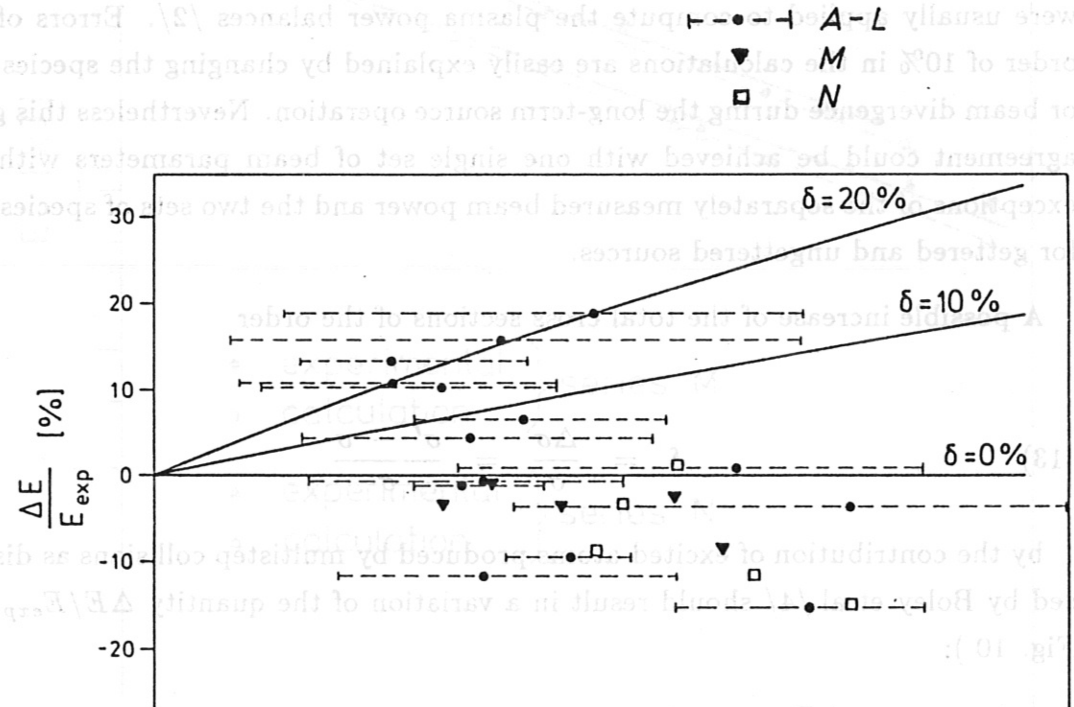

Despite of the large scattering of the data points in the range -15 % $\leq$ $\Delta E/E_{exp} \leq$ 20 % an increase of the total cross-section in the order of 20 % should be detectable at line densities exceeding $10^{15}\ cm^{-2}$. But the lack of a systematic variation of this quantity with inreasing line density limits the contribution of the multistep collision processes to less than 20 % under W VII-A conditions. This finding does not contradict the model reported in Ref. /4/ within the error estimation.

V. Conclusions

From the good agreement between measured and calculated shinetrough of the Wendelstein VII-A injection it is concluded that the NEUDEN code, which is used after some minor modifications, correctly describes the absorption of a neutral beam in a given target plasma in the energy range up to 30 keV. Although the compared quantity, the energy deposited on the torus calorimeter, is only a global one, integrated over space and time during the pulse, this agreement confirms the result of the sensitivity study for NEUDEN that an accuracy of better than 20% for the calculation of the power density or particle density of a neutral beam inside or behind a plasma is possible .

The lack of a systematic deviation from the experimental points indicates that there is no need for additional multistep collision processes as discussed by Boley et al./4/, at least at beam energies below 30 keV. Nevertheless it should be mentioned that such a process would only significantly contribute, i.e. more than 20%, to the cross-sections at higher energies.

Acknowledgements

The initiation of this work by E. Speth is gratefully acknowledged. The author also expresses his thanks to his colleagues of the W VII-A team, H. Renner, G. Kühner and E. Würsching, for supplying the necessary informations on the plasma shots analysed.

References

/1/. W VII-A Team , NI Team, *Neutral Beam Heating in the W VII-A Stellarator*, "Proc. 2nd Int. Symp. on Heating in Toroidal Plasmas, Vol II", 1980, p. 789.

/2/. W VII-A Team , NI Team, *Neutral Injection Heating in the Wendelstein VII-A Stellarator*, "Proc. 9th Int. Conf. on Plasma Physics and Contr. Nucl. Fus., Vol II", 1982, p. 241.

/3/. F. P. Penningsfeld, *Computation of the density distribution of fast injected neutral beam particles by the program NEUDEN*, IPP report 4/229 (Nov 1986).

/4/. C. D. Boley, R. K. Janev, D. E. Post, *Enhancement of the neutral beam stopping cross section in fusion plasmas due to multistep collision processes*, Phys. Rev. Lettr. **52(7)** (1984), p. 534.

/5/. W. Ott, F. P. Penningsfeld, D. Cooper, K. Freudenberger, et al., *Experience with the Wendelstein VII-A neutral injectors*, "Proc. 9th Symp. on Eng. Probl. on Fus. Res., Vol I", Oct. 1981, p. 779.

/6/. W. Ott , K. Freudenberger, F.-P. Penningsfeld, F. Probst and R. Suess, *Reduction of the impurity concentration of an intense hydrogen beam*, Rev. Sci. Instr. **54(1)** (1983), p. 50.

/7/. D. L. Galbraith, T. Kammash, *Analytical approximations to the rate coefficients for charge exchange and ionisation of neutral beams*, Nucl. Fus. **19(8)** (1979), p. 1047.